

Amass

Advanced manufacturing for the assembly of structural steel

Shemshadian, Mohammad E.; Schultz, Arturo E.; Le, Jia Liang; Labbane, Ramzi; Laefer, Debra F.; Al-Sabah, Salam; Truong-Hong, Linh; Huynh, Minh Phuoc; McGetrick, Patrick; Martin, Tony

DOI

[10.1061/\(ASCE\)SC.1943-5576.0000516](https://doi.org/10.1061/(ASCE)SC.1943-5576.0000516)

Publication date

2021

Document Version

Accepted author manuscript

Published in

Practice Periodical on Structural Design and Construction

Citation (APA)

Shemshadian, M. E., Schultz, A. E., Le, J. L., Labbane, R., Laefer, D. F., Al-Sabah, S., Truong-Hong, L., Huynh, M. P., McGetrick, P., Martin, T., & Matis, P. (2021). Amass: Advanced manufacturing for the assembly of structural steel. *Practice Periodical on Structural Design and Construction*, 26(1), Article 04020052. [https://doi.org/10.1061/\(ASCE\)SC.1943-5576.0000516](https://doi.org/10.1061/(ASCE)SC.1943-5576.0000516)

Important note

To cite this publication, please use the final published version (if applicable).
Please check the document version above.

Copyright

Other than for strictly personal use, it is not permitted to download, forward or distribute the text or part of it, without the consent of the author(s) and/or copyright holder(s), unless the work is under an open content license such as Creative Commons.

Takedown policy

Please contact us and provide details if you believe this document breaches copyrights.
We will remove access to the work immediately and investigate your claim.

AMASS: Advanced Manufacturing for the Assembly of Structural Steel

Mohammad E. Shemshadian¹, Arturo Schultz¹, Jia-Liang Le¹, Ramzi Labbane¹, Debra Laefer^{2,3},
Salam Al-Sabah³, Linh Truong-Hong⁴, Minh Huynh³, Patrick McGetrick⁵, Tony Martin⁵, and
Pantelis Matis⁵

¹*Department of Civil, Environmental and Geo- Engineering, University of Minnesota, Twin Cities, USA*

²*Center for Urban Science and Progress and Department of Civil and Urban Engineering, Tandon School of
Engineering, New York University, New York, USA*

³*School of Civil Engineering, University College Dublin, Dublin, Ireland*

⁴*Dept. of Geoscience and Remote Sensing, Delft Univ. of Technology, 2628 CN Delft, Netherlands*

⁵*School of Natural and Built Environment, Queen's University Belfast, Belfast, Northern Ireland*

Abstract

This paper describes a collaborative project between researchers in the US, Ireland, and Northern Ireland (UK) to investigate advanced manufacturing techniques for the creation of a new class of ‘intermeshed steel connections’ that rely on neither welding nor bolting. To date, advanced manufacturing equipment has only been used to accelerate traditional processes for cutting sheet metal or other conventional fabrication activities. Such approaches have not capitalized on the equipment’s full potential. This project lays the groundwork to transform the steel building construction industry by investigating the underlying science and engineering precepts for intermeshed connections created from precise, volumetric cutting. The proposed system enhances the integration between design, fabrication, installation, and maintenance. Fully automated, precise, volumetric cutting of open steel sections introduces intellectual challenges regarding the

24 load-transfer mechanisms and failure modes for intermeshed connections. The research activity
25 addresses knowledge gaps concerning the load resistance and design of steel systems with
26 intermeshed connections. Physical tests and finite element modeling were used to investigate the
27 mechanics of intermeshed connections including stress and strain concentrations, fracture potential
28 and failure modes, and to optimize connection geometry.

29 **Keywords:** Steel Connection, Intermeshed, Plasma, Waterjet, Finite Element Modeling,
30 Experiment.

31

32 **1. INTRODUCTION**

33 Despite field welding and bolting being time-consuming and/or expensive, the steel
34 building market has not developed any new universally applicable structural steel connection
35 systems since before World War II. To achieve improved construction efficiency and heightened
36 material reuse, computer controlled, advanced manufacturing techniques in high-definition
37 plasma, laser and waterjet cutting could be exploited [1]. This paper envisions the harnessing of
38 those technologies to create an entirely new class of “intermeshed” steel connections.

39 Precise cutting of steel makes it possible to create the notches in beam flanges and web that
40 can intermesh with other beam parts or external connectors, like puzzle pieces. This technique
41 could radically change how structural steel is fabricated, assembled, deconstructed, and reused [2].
42 Without relying solely on bolting or welding to assemble a connection in the field, the simplicity
43 and efficiency of the construction process may be significantly improved. To date, this class of
44 fabrication equipment has only been used to accelerate traditional processes for cutting sheet metal

45 or other conventional fabrication activities (e.g. cutting instead of drilling holes). Such approaches
46 have not capitalized on the equipment's full potential.

47 Because assembly and inspections costs at a construction site are high for welded and
48 bolted connections, the intermeshed connection offers the potential for a lower cost connection,
49 even though manufacturing costs are likely to be higher. There is also the potential for life cycle
50 savings as deconstruction costs would be significantly lower as an intermeshed connection can be
51 designed specifically for disassembly and reuse. However, unlike traditional bolted or welded
52 connections, where the industry has more than 100 years of experience, precise cutting of steel for
53 an intermeshed connection is not yet part of the culture or expectations.

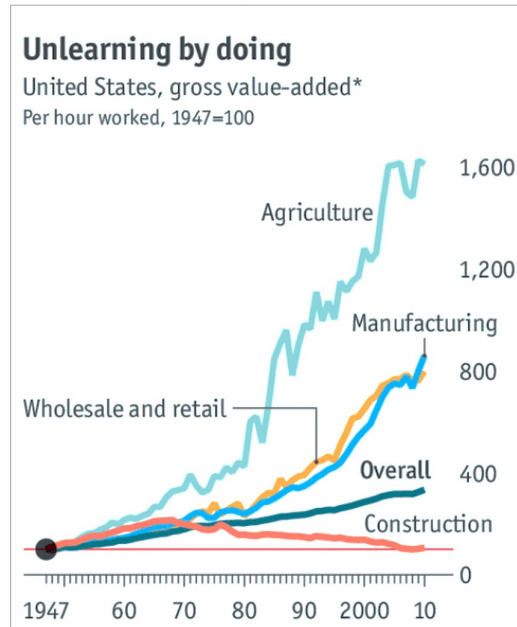
54 While maintaining the original concept, different details can be proposed for the
55 intermeshed connection. In this paper, two variations of the intermeshed connection are presented
56 and studied in the following sections.

57

58 **2. AUTOMATION IN STEEL CONSTRUCTION**

59 Construction is one of the largest sectors in the world economy and approximately 7% of
60 the world working population is employed by construction-related services. However, the
61 productivity of this industry has barely grown for decades compared to other industries. Since
62 1945 in the United States, the overall productivity in all sectors has grown by 400 percent, while
63 productivity in construction has not increased at all (Fig. 1) [3]. One of the reasons for this
64 underperformance is that the construction industry is highly regulated, and the common techniques
65 have not been updated in years. Steel construction as a subcategory of the construction sector has
66 also suffered from restrictive design specifications, underinvestment in skills development, and

67 insufficient innovation. Consequently, commonly used alternatives for steel connections have not
68 been developed in the past 50 years.



69

70

Fig. 1: Productivity of different sectors in United States [3]

71

72

73

74

75

76

Developing new construction methodologies such as prefabricated volumetric construction and digital technologies can further facilitate off-site fabrication. Specifically, in the steel construction industry, ‘advanced manufacturing techniques’ such as plasma cutting and waterjet cutting could be utilized. These fully automated cutting techniques could enhance the fabrication process and consequently increase construction productivity.

77

78

79

80

Traditionally, steel plates are cut using saws or oxy-fuel for structural purposes. These techniques are mainly applied manually, which results in highly variable speed and accuracy. The new computer-controlled cutting techniques would help improve the precision of fabrication, and by combining them with robotic arms, faster and more flexible operation would ensue. Although

81 a variety of options is available based on project needs, this research focuses on the implementation
82 of plasma and waterjet cutting in steel fabrication.

83 High definition plasma cutting is a thermal process achieved through a concentrated high-
84 speed plasma stream [4]. The plasma stream is extremely hot at up to 30,000 K, and it cuts through
85 the material by melting it [5]. The plasma cutter may be attached to a robotic arm with multiple
86 degrees of freedom, giving it unlimited possibilities regarding the position and configuration of
87 the cut surfaces. Waterjet cutting can also be used to precisely cut various materials, including
88 structural steel. High pressure waterjets with abrasive additives are used to cut the material by
89 eroding away at the surface [4]. This form of cutting may be a desirable alternative to plasma
90 cutting due to its lower energy demand and lack of thermal effects on the cut material [6].
91 Moreover, waterjet provides more precise cuts in a wider range of plate thickness. As an emerging
92 technology with certain advantages over other cutting methods, use of waterjet cutting may
93 become more widespread in the future.

94 Using these cutting techniques can open up an opportunity to create an alternative steel
95 connection that relies on intermeshed (i.e. interlocked) components, instead of regular welding or
96 bolting techniques. In this class of connection, the force transfer is achieved through direct contact
97 bearing of multiple, precisely shaped surfaces of the interlocking elements. However, due to the
98 absence of welds or bolts in the connection detail, it is likely that the intermeshed connection
99 would not behave as a fully rigid connection. Therefore, the effects of implementing such
100 connections needs to be evaluated by investigating the response of steel frames equipped with
101 intermeshed connections.

102

103 **3. MOMENT FRAMES WITH INTERMESHED CONNECTION**

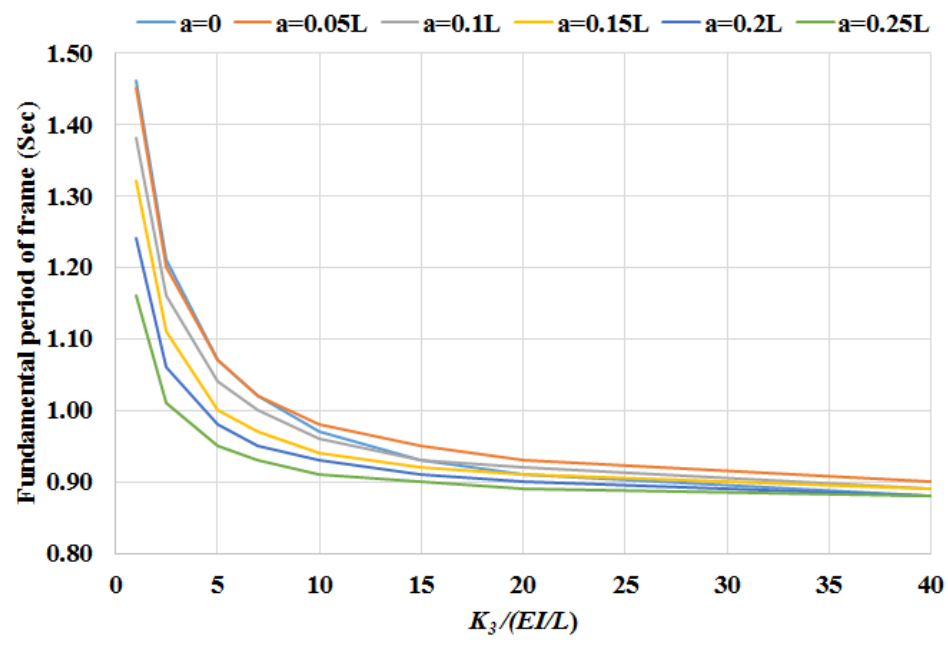
104 Structural connections are frequently assumed as ideally pinned or fixed in numerical
105 modeling. However, these assumptions do not accurately represent the behavior of the intermeshed
106 connection. In reality, the connection stiffness is expected to be somewhere between the two
107 extremes due to the cuts in section which causes discontinuity in the load path. Therefore, in the
108 case of this connection, a spring with assigned stiffness is more representative and helps achieve
109 reasonable accuracy in the frame responses. However, inclusion of the connection stiffness in the
110 analysis affects the distribution of the internal forces and deformations in the frame and needs
111 further investigation. To determine the influence of connection rigidity on frame response, a series
112 of linear analyses was conducted on variety of frames with different connection properties. The
113 goal is to understand the influence of connection rigidity on frame overall stiffness as well as stress
114 distribution in different frame members. At the end of this step, practical recommendations will
115 be provided on ‘optimal locations’ and ‘suitable stiffness range’ for the intermeshed connection.

116 Members and connections in gravity framing are typically designed to resist vertical loads.
117 However, most building structures are subjected to lateral loads with wind and seismic forces being
118 the most common. Even though lateral load resisting systems such as structural cores and braced
119 frames are often used to resist these loads, the gravity frames must undergo the associated lateral
120 displacements with little or no loss in vertical load capacity. This ability can be quantified by
121 determining the changes in internal forces (moment, shear, and axial forces) that occur under the
122 imposed lateral drifts. Large increases in these internal forces would be indicative of gravity
123 framing that would be at risk.

124 This aspect of the research utilized two-dimensional (2D) pushover analysis with
125 commercial software SAP2000. Translational (K_1 , K_2) and rotational (K_3) stiffness of the
126 intermeshed connection were idealized as elastic springs in linear elastic models of prototype steel
127 frames and the models were analyzed under various load schemes. First, gravity (dead and live)
128 load was applied, and then, the frames were pushed to 2% of their height to simulate the maximum
129 expected drift from the lateral force. A range of 2D frames with different geometries for 3-story
130 and 9-story frames, with span-to-height ratio of two and three, were considered. Changes in
131 internal forces are affected by the location and stiffness of the spring. Therefore, to find the optimal
132 location of the connection, the position of the connections (a) in the span length (L) was changed
133 from zero to 0.25 of L gradually (i.e., $a/L = 0, 0.05, 0.1, 0.15, 0.2, \text{ and } 0.25$). Since the detail of the
134 connection had not been defined at this stage, the translational and rotational stiffness coefficients
135 of the connection were unknown. Therefore, a wide range of spring stiffness was assumed: 20, 10,
136 5, 1, 0.5, 0.2, and 0.1 times of the beam stiffness, which were defined for the three structural actions
137 as follows. Axial stiffness (EA/L), shear stiffness (GA/L), and flexural stiffness (EI/L) were
138 calculated using geometric properties of the beam section (A and I), beam length (L), and elastic
139 material properties of the structural steel (E and G). To fully cover the range of selected variables
140 in frames, more than 300 frames were modeled and analyzed.

141 Rotational stiffness of the connection, K_3 , was found to affect frame lateral stiffness (Fig.
142 2) and beam deflection drastically, especially when the connections are located near the beam ends.
143 According to AISC recommendations, the minimum value for rotational stiffness of a connection
144 to be categorized as fully rigid is 20 ($K_3 \geq 20EI/L$). Fig. 2 also shows that beyond the same stiffness
145 limit, increasing rotational stiffness produces no appreciable change in structural response,
146 regardless of the connection location. Considering $K_3 \geq 20EI/L$ (i.e. fully rigid frame) to be the

147 benchmark case, comparison could be performed to learn the effect of reduction in the connection
 148 rotational stiffness on the fundamental period of the frame. Fig. 2 shows changes in the frame
 149 fundamental period based on changes in the ratio of connection rotational stiffness to beam flexural
 150 stiffness ($K_3 / (EI/L)$). It can be seen that although a reduction of this ratio below 20 increases the
 151 fundamental period of the frame, the increases are limited to a range of 10% to 20%, even when
 152 the ratio drops to 10 and 5 respectively. This is a promising discovery, since connection rotational
 153 stiffness values of $5EI/L$ to $10EI/L$ in the intermeshed connection may be possible without
 154 requiring a cumbersome geometry.



155
 156 Fig. 2: Effects of connection rotational stiffness (K_3) and connection location (a) on fundamental
 157 period of the frame
 158

159 As previously defined, a benchmark case is a frame in which all the connections are fully
 160 rigid and located at beam ends, and all the beams and columns are continuous. Variant frame cases

161 consist of new connection locations and/or new connection rotational stiffness values, but the same
 162 beams and columns section sizes. In the next stage of frame analysis, the maximum P - M (axial
 163 load combined with moment) stress ratio in each frame was calculated based on the following
 164 equation:

165 Stress ratio = $\frac{P_r}{P_a} + \frac{M_r}{M_a}$

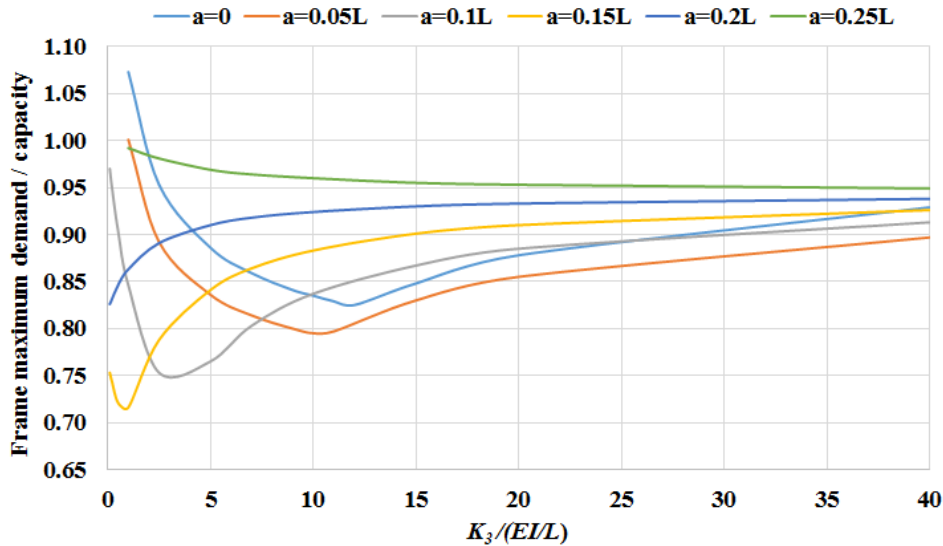
166 Where P_r and M_r are required axial and flexural strength, and P_a and M_a are available axial
 167 and flexural strength respectively. Fig. 3 shows that the optimum stress ratio exists at a smaller
 168 stiffness ratio, when the connection was located closer to the beam ends. Therefore, it is easier to
 169 control the stress ratios of the beam, as the connection is located closer to the beam ends. The
 170 optimal location of the connection was defined at $0.1L$ from the beam ends. Having the connection
 171 at this location led to smaller beam stress ratios for a wider range of stiffness ratio, which is a result
 172 of a more uniform moment distribution in the beam length. It also needs to be mentioned that the
 173 obtained ration ($0.1L$) is compatible with the current codes recommendations for the plastic hinge
 174 length. Table 1 shows the frame responses when the intermeshed connection was placed at $0.1L$
 175 from the span ends. Selecting a connection rotational stiffness of $5EI/L$ or $10EI/L$ (or any value in
 176 between), would result in reduction in the frame P - M stress ratios while the fundamental period
 177 undergoes a slight increase, which means the frame lateral stiffness is not dropping significantly.
 178

179 Table 1: Change of the frame responses when $a=0.1L$

K_3	$2EI/L$	$5EI/L$	$10EI/L$
Reduction in P - M stress ratios	25%	23%	16%

Increase in fundamental period of frame	35%	16%	7%
---	-----	-----	----

180



181

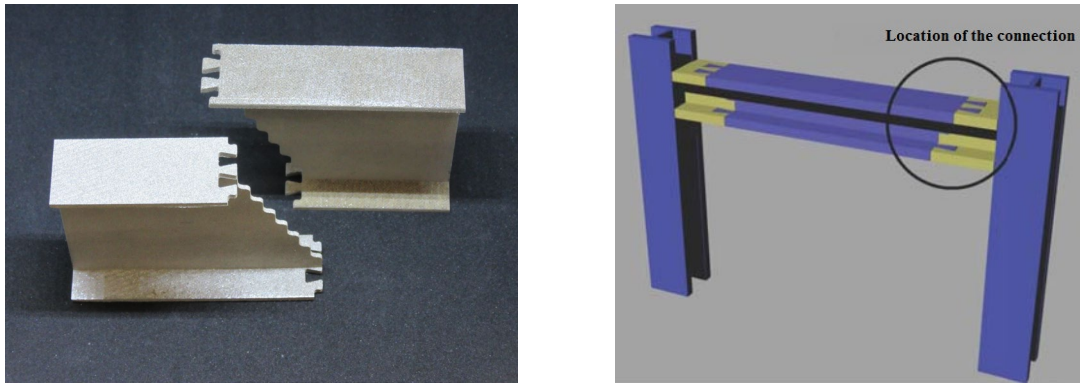
182 Fig. 3: Effects of connection rotational stiffness (K_3) and connection location (a) on beam stress
 183 ratio

184

185 4. FRONT-INTERMESHED CONNECTION

186 The first conception was a relatively simple intermeshed connection denoted as the “Front-
 187 Intermeshed Connection” [7]. This connection is composed of three-dimensional interlocking
 188 through the top and bottom flanges and through the web. The flanges carry the tension and
 189 compression resulting from the bending moment at the connection while the web carries the shear
 190 force. The connection transfers shear and compression from one beam section to the next through
 191 direct contact bearing of multiple, precisely shaped faces (Fig. 4a). The arrangement is ideally
 192 suited for connecting beams at or near ideal inflections points to create gravity load framings. For

193 practical use of this new type of connection, understanding its mechanical behavior, especially in
194 terms of the load carrying capacity under mixed mode loading scenarios is essential.



(a) Idealized connection in printed stainless steel (b) Assembly of the connection in a frame

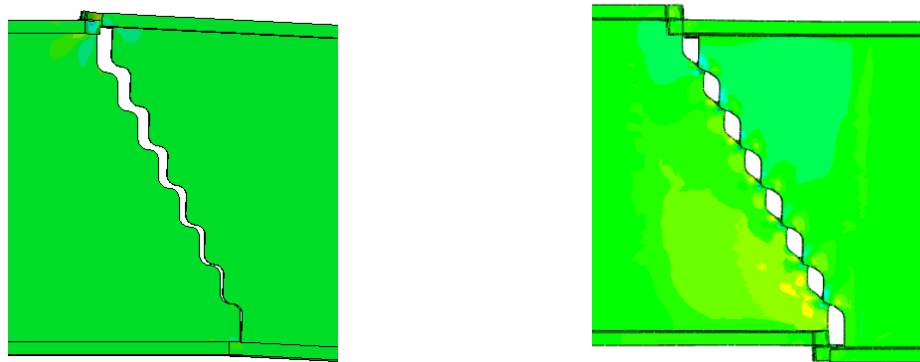
195 Fig. 4: Front-intermeshed connection

196

197 Load is transferred between flanges through bearing and friction via the intermeshed
198 dovetails of the flanges. The connection has the advantage of simplicity and requires no additional
199 parts to create the flange connection, although a locking mechanism can be added to provide
200 resistance against uplift. However, field-assembled locking connections are unlikely to be able to
201 fully transmit the flexural, axial and shear capacities of the connected steel sections and may reduce
202 the corresponding stiffness components of a continuous steel member, due to interruptions in the
203 load path.

204 The stepped web connection allows for easy site assembly, as the middle beam part can be
205 dropped from above, in a method similar to current practice. In Fig. 4b, the ends shown in yellow
206 are shop welded as stubs to the column. No other welding is required, and bolting is fully avoided
207 in this configuration. The main drawbacks to this type of connection are the tightness of the
208 tolerances and the lack of adjustability in the erection process.

209 To better understand how this type of precise interlocking performs structurally, initial
210 laboratory testing was conducted for the two-dimension meshed “dovetails” [8]. Based on the
211 success of those initial tests, a three-dimensional numerical model was created in Abaqus [9].
212 Finite element analyses were performed under different load combinations to investigate the
213 general behavior, failure modes, and peak capacity of the connection. Under flexure, the
214 connection shows a uniformly monotonic behavior with a relatively low flexural resistance. Failure
215 occurs when the dovetails on one side of the top flange slip out of the sockets on the other side
216 (Fig. 5a), so there is no capacity to carry tension force, which means no moment capacity can be
217 developed. Moreover, in the case of combined tension and shear, the presence of the shear force
218 causes relative vertical movement between the two sides of the connection and, consequently, the
219 flanges slip out of their intermeshed positions. When this phenomenon happens (Fig. 5b), there is
220 no component to resist tension, and the connection fails.



(a) In pure flexure, top flange slips out

(b) In combined tension and shear, top and bottom flanges slip out

221 Fig. 5: Performance of the front-intermeshed connection under different load conditions

222

223 Considering the connection configuration and the results of the finite element analyses, the
224 front-intermeshed connection cannot generate sufficient strength and stiffness for effective use in
225 practice. Following current code standards and based on the results from the finite element studies,

226 the front-intermeshed connection shows limited stiffness, strength, and ductility. So, it is classified
227 as a non-ductile and partially restrained connection [10,11]. This classification is due to the cuts
228 in the flanges which reduce load carrying capacity in tension and, consequently, the moment
229 significantly. Therefore, the front-intermeshed connection is not recommended for use where
230 demands for 1) large moments, 2) large moments in combination with large shears, and 3) axial
231 tension are possible.

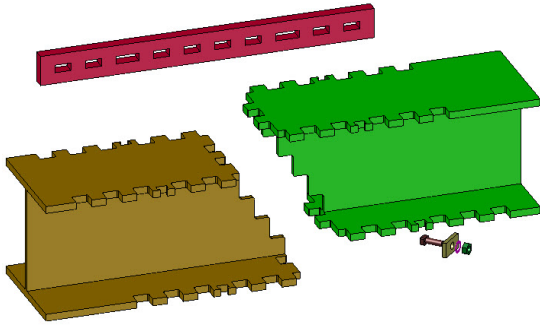
232

233 **5. SIDE-INTERMESHED CONNECTION**

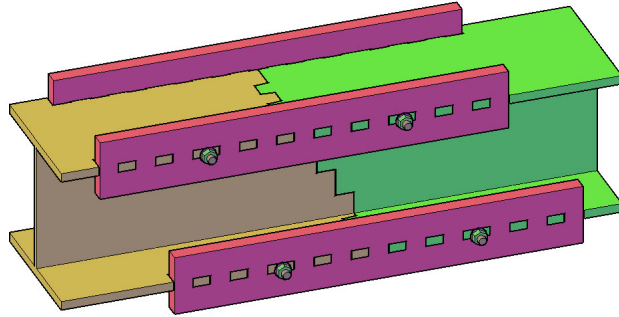
234 Given the limitations of the front-intermeshed connection in transferring loads, especially
235 when combined loads are present, and the requirement for strict tolerances, another alternative of
236 the intermeshed connection is proposed [12]. The “Side-Intermeshed Connection” employs
237 intermeshed external connectors to transfer flanges tension and compression forces.

238 At this step, two different versions of side-intermeshed connection were developed. The
239 ‘original conception’ (Fig. 6) sought to meet the original goals of requiring no welding nor bolting,
240 while maximizing erection speed and construction tolerance. Meanwhile, the modified version
241 (Fig. 7) was developed for greater acceptance in the construction industry. The remainder of the
242 paper focuses on the modified side-intermeshed connection.

243



(a) 3D Exploded view

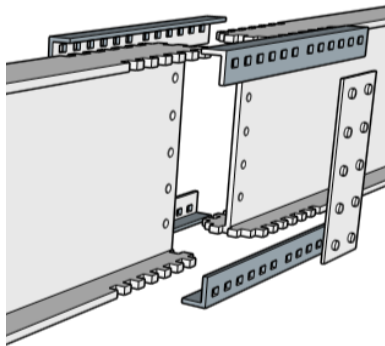


(b) 3D View of assembled connection

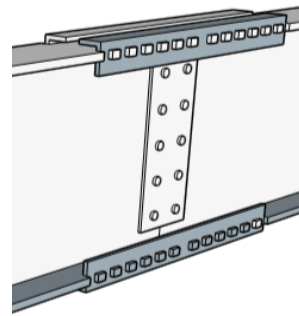
Fig. 6: Side-intermeshed connection (original conception)

244

245



(a) 3D Exploded view



(b) 3D View of assembled connection

Fig. 7: Side-intermeshed connection (modified version)

246

247

248 In this connection, flange edges are cut to create a set of tooth-shape notches (i.e. ‘teeth’).

249 To connect different sides of the beam, an angle is used on each edge with rectangular holes

250 (sockets) which match the teeth (see Fig. 7). Having the beam flanges connected, the section will

251 be able to transfer moments via the connector angles. However, for shear transfer, a pair of regular

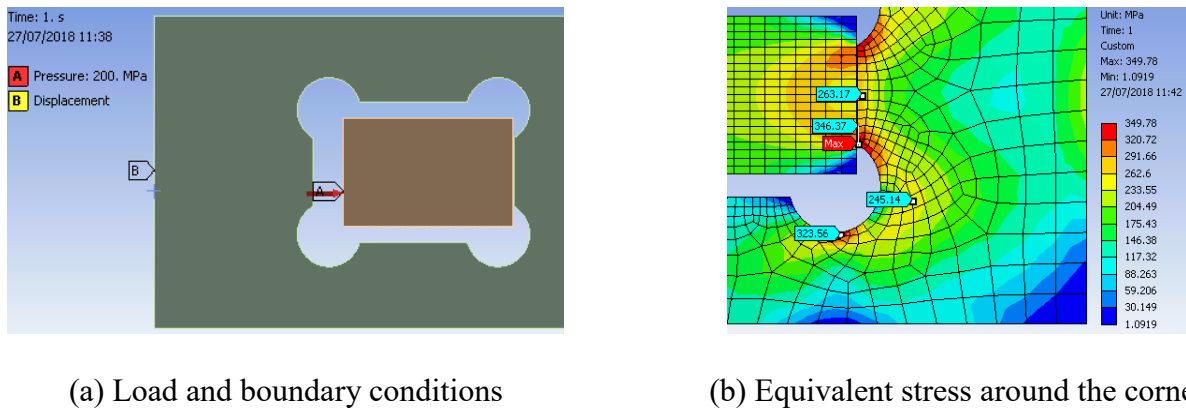
252 shear plates are bolted to the beam web.

253 The side-intermeshed connection allows larger tolerances and easier fabrication, which

254 leads to a better potential for wider acceptance in practice. However, one potential concern related

255 to this connection is the stress concentration at the sharp corners of the angle sockets. Depending

256 on the length-to-width ratio of the angle sockets, previous studies have shown that the stress
257 concentration factor can be up to five [13] which can result in a pre-mature rupture. To avoid any
258 undesirable failure modes, circular holes were added to the sharp corners in the angle sockets. A
259 finite element model proved the effectiveness of such a change by reducing the stress concentration
260 factor to 1.7. Fig. 8 shows the configuration of the socket and the resulting stress.



261 Fig. 8: Finite element analysis on the effect of the shape on the stress concentration around the
262 socket

263

264 5.1. Design procedure and analysis method

265 A procedure was developed for analyzing and designing the modified side-intermeshed
266 connection (Fig. 7) using fundamentals of structural mechanics. The design procedure was based
267 upon the requirements of the current American steel design standards [10,14,15] to ensure the
268 practicality and sufficiency of the connection.

269 In traditional structural design, the connection would be proportioned after the appropriate
270 beam sections have been selected to resist a given combination of loads. Thus, some properties
271 such as the beam section size and beam material properties were assumed to be determined here,

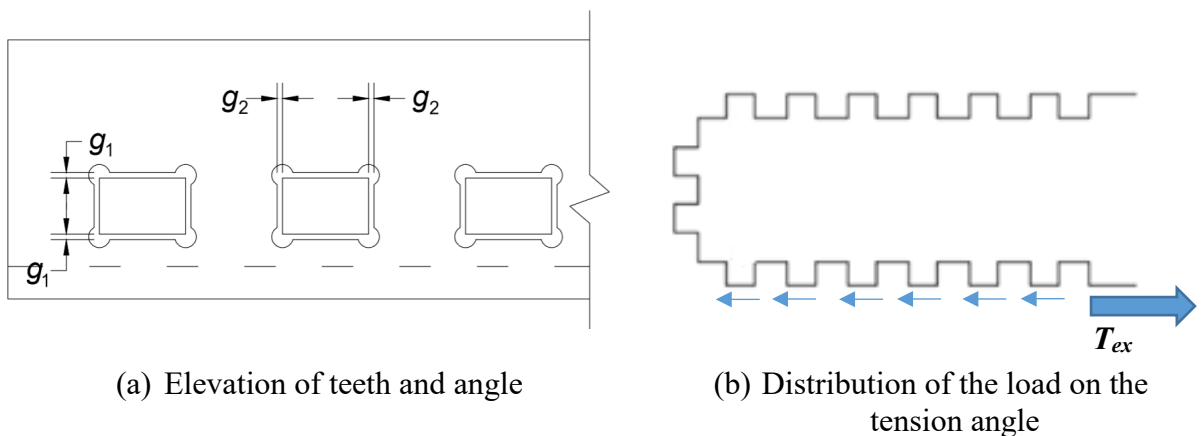
272 prior to the connection design. This means that the thickness of the teeth is equal to the beam
273 flange thickness and should not be adjusted when the connection is being designed. Other
274 geometric parameters, such as the length of a single tooth, the number of teeth, and the size of the
275 angles are dependent upon one another and must be chosen iteratively during the design of the
276 connection for moment.

277 Another basic assumption in this design procedure is that the connection will transfer the
278 moment and shear loads separately; meaning the angles will take all the load due to moment, and
279 the plates will take all the load due to shear. Therefore, the design procedure of side-intermeshed
280 connection combines two different procedures: ‘shear design’ and ‘moment design’. The shear
281 design follows a conventional shear tab design according to the AISC recommendations [10]
282 which results in the selection of suitable shear plates and bolts. Moment design, however, requires
283 several steps and likely multiple iterations due to the more complex load transfer mechanism of
284 the intermeshed segments. The moment design process will be discussed in detail in the following
285 paragraphs.

286 As mentioned previously, these connections are not recommended for placement near the
287 location where maximum moment will be experienced. Therefore, the full plastic capacity of the
288 beam section is not required to be developed by the connection, and a fraction of this capacity
289 becomes a design choice. In this research, one-third the plastic moment capacity of the beam was
290 selected as the design moment (M_d). As previously stated, one of the basic assumptions of this
291 design procedure is that the angles take all the moment load without any contribution from other
292 connection elements. The design moment, M_d , transfers through the angles in form of a force
293 couple, i.e. compression in the top angles, P_d , and tension in the bottom angles, T_d (assuming
294 positive bending moment). Assuming all four angles and the corresponding flange teeth are

295 identical, each top angle takes $P_d/2$ and each bottom angle takes $T_d/2$ from the load share. Then,
 296 the angles are proportioned at these demand levels for ‘yielding at the gross section’ as well as
 297 ‘rupture at the net area’ based upon the AISC recommendations [10].

298 Dimensions for the circular cuts (R) at socket corners were chosen so that an adequate
 299 amount of stress could be relieved without significantly reducing the angle cross section.
 300 Dimension of the sockets in the angles are a function of the teeth sizes plus the considered
 301 tolerances, g_1 and g_2 , on top/bottom and left/right side of the teeth respectively, as shown in Fig.
 302 9a. It is important to notice that at this point, the horizontal dimension of the teeth was still
 303 unknown (the vertical dimension equals the beam flange), therefore, an initial value must be
 304 assumed. This value was later adjusted during the teeth strength design which will be discussed in
 305 the following paragraph. The adjusted value would change the socket size and consequently affect
 306 the angle design; thus, this design procedure needs several iterations until the sizes converge.



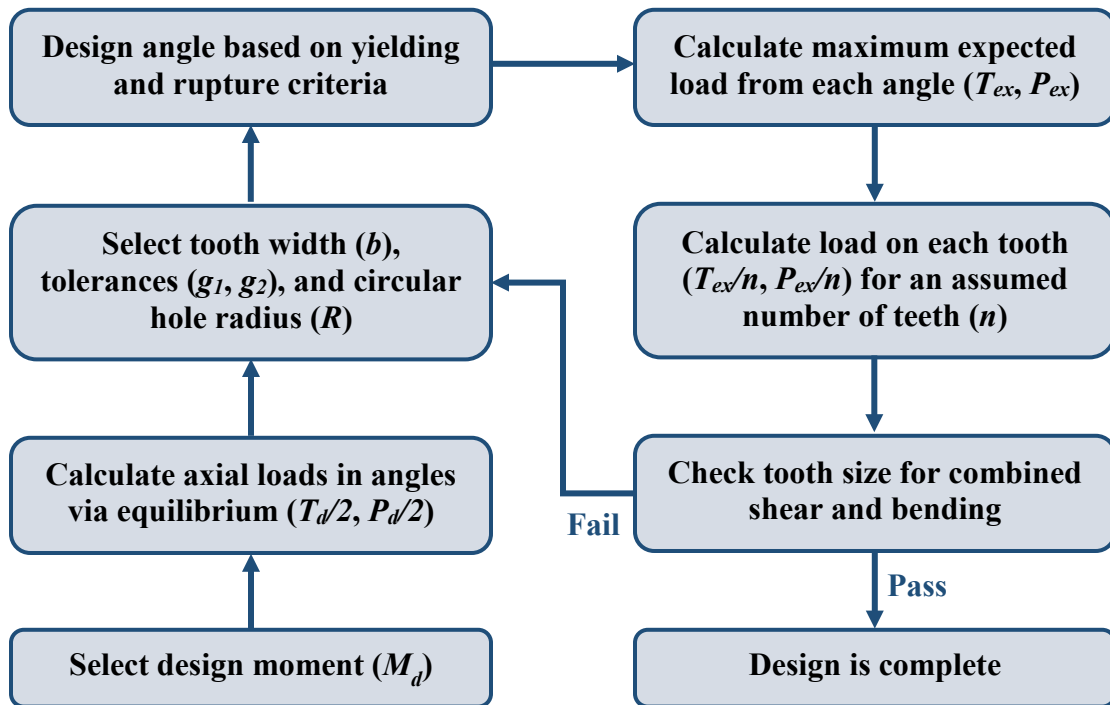
307 Fig. 9: Detail of geometry and load path in the connection

308

309 In this step of the design, the teeth are sized for the maximum expected forces based on
 310 connector angle capacity, which is symbolized as T_{ex} for the tension angle and P_{ex} for the

311 compression angle. This concept, known as ‘Capacity Design’, assures that the failure in the angles
 312 occurs before the teeth failure. Such mechanism is desirable since the replacement of the angles is
 313 easy and fast following any case of damaging overload. Assuming all the teeth have equal
 314 contribution in transferring the angle load, each tooth has to bear T_{ex}/n (or P_{ex}/n), where n is the
 315 number of the teeth on one side of the connection (see Fig. 9b). Therefore, each tooth needs to be
 316 checked for the combined shear and moment stresses caused by the external load.

317 Once all geometries and material properties are stated, the capacity of the connection may
 318 be checked against the demand. The size of the connection components may then be increased or
 319 decreased to produce an adequate and optimally efficient configuration. Several iterations may be
 320 necessary to develop an arrangement that is appropriate for a given moment. The flowchart shown
 321 in Fig. 10 helps understand the step-by-step process of the moment design for the side-intermeshed
 322 connection.



323

324 Fig. 10: Moment design of side-intermeshed connection

325

326 **5.2. Fabrication process and challenges**

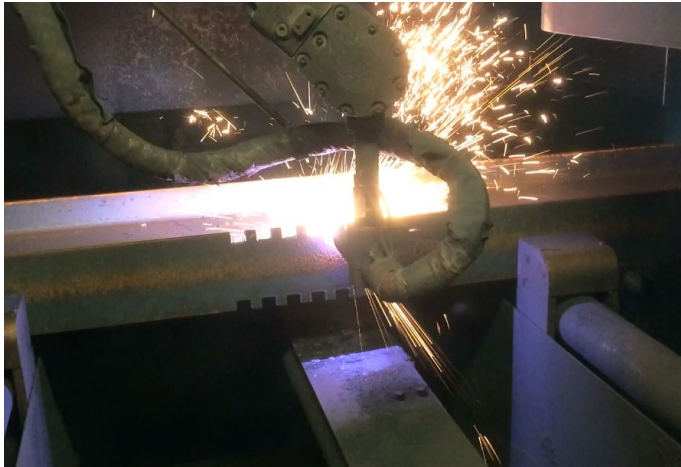
327 An experimental program at the University of Minnesota aimed to investigate the
328 performance of the side intermeshed connection under different load conditions. For this purpose,
329 two beam sizes, W18x46 and W21x57, were selected from commonly used members based upon
330 engineering judgment. The intermeshed connections were designed for these beams according to
331 the procedure described in the previous section, which resulted in the angle sizes $L2\frac{1}{2}\times 2\times 3/8$ and
332 $L3\times 2\times 3/8$ respectively.

333 The side-intermeshed connection was developed primarily to offer greater ease of
334 fabrication and assembly than the front-intermeshed connection. Larger tolerances were included
335 in this configuration to increase the adjustability of the connection, allow connecting elements to
336 be placed safely and easily, and accommodate imperfections in the connected members. A
337 tolerance of 1.6 mm was specified for all the connection components, except for the circular holes
338 in the angle sockets, which needed a more precise cut of 0.8 mm. These were the precision the
339 cutting machine needed to have in order to meet the project requirements. Furthermore, it had to
340 be able to penetrate the thickest steel element (16.5 mm for the beams and 9.5 mm for the angles),
341 while maintaining the required precision level.

342 Regarding the precise geometry of the side-intermeshed connection, high-definition
343 plasma and waterjet cutting were selected for manufacturing of different parts based on the project
344 need. Both techniques are capable of cutting structural steel with high precision. Plasma cutting,
345 which works based on a ‘melt and blow’ mechanism, can be used to cut metal plates with the

346 maximum thickness of 60 mm with 0.25-0.4 mm precision. However, making cuts using plasma
347 is a relatively slow process and the cut finish quality is average. Waterjet cutting, on the other
348 hand, is a very fast technique that provides an excellent smooth cut finish with high precision
349 (0.05-0.2 mm) in 75 mm thickness [16,17]. This technique relies on ‘erosion’ cutting method
350 which avoids the formation of ‘heat affected zone’ and keeps the material properties uniformly
351 distributed. Although these advantages make waterjet an attractive cutting technique to use, it is
352 more costly than plasma cutting. Furthermore, it is difficult to integrate waterjet technology into a
353 typical steel fabrication production line [18].

354 Local and regional fabricators were contacted to investigate the feasibility of fabricating
355 the beams, angles, and shear plates for the side-intermeshed connection. Plasma cutting was
356 selected for the fabrication of the beams and shear plates. The manufacturer used a Python X
357 Robotic CNC (Computer Numerical Control) Plasma Cutting System for their fabrication. The
358 plasma cutting of one of the beam specimens is shown in Fig. 11a. Although plasma cutting could
359 guarantee the precision of 1.6 mm required for the beams, it could not achieve the 0.8-mm
360 precision in the angles sockets. Therefore, waterjet technique was selected to fabricate the angles.
361 The manufacturer used an OMAX A-Jet waterjet cutting machine to cut the angles and
362 successfully reach the specified precision. Another reason for using waterjet cutting for the angles
363 was to prevent heat affected zones to build around the sockets. Large plasticity was expected to
364 occur in the angles and a heat affected zone could cause brittle fracture through a potential change
365 in the material properties. Fig. 11b shows waterjet cutting of one of the angles.



(a) Plasma cutting performed by an industrial robot



(b) Waterjet CNC cutting machine

Fig. 11: Advanced cutting techniques

366

367

368

369

370

371

372

373

374

375

376

The required capability to manufacture the specimens was found at steel fabrication shops near the University of Minnesota. The fabricators were able to meet the needs of the projects without significant changes to their fabrication procedures. Once the specimens arrived in the laboratory, they were measured with calipers to check the accuracy of the fabrication. On the beams, every single tooth was measured, and the maximum deviation was found to be 1.4 mm which is within the specified tolerance value of 1.6 mm. Every socket on every angle was also measured. The maximum deviation in both the width and the height of each socket was found to be 0.4 mm which is well within the allowable tolerance value of 0.8 mm. The measurements verified that both plasma cutting and waterjet cutting are acceptable for the precision required for the side-intermeshed connection.

377

5.3. Structural performance - experimental study

378

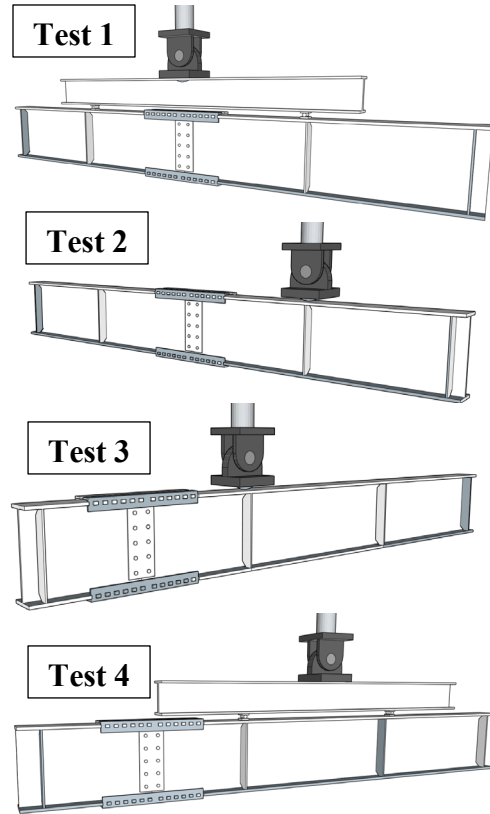
379

380

Four full-scale beam specimens with intermeshed connection were designed using the design procedure in Section 5.1, and fabricated using precise, fully automated cutting techniques. An experimental testing program was conducted with these specimens to study the behavior of

381 intermeshed connections under gravity loads. The validity of the proposed design procedure also
382 needed to be verified with experimental testing in order to gain acceptance for adoption by design
383 and construction codes.

384 The experimental work involved four major-axis beam tests with the intermeshed
385 connection located along the beam span and in two different locations. In the first two specimens,
386 the connection was in the middle of the beam, while in the other two specimens, it was located at
387 the beam end (Fig. 12). This change in location was to study the effect of connection location on
388 the global behavior of the specimen. In the first test, the connection was placed in the pure moment
389 region, whereas in the other three tests, the connection was subjected to a combination of bending
390 moment and shear forces with different ratios (see Table 2). Structural steel used for the beam and
391 angles were Grade 50 and Grade 36, respectively, as specified by the American Society for Testing
392 and Materials (ASTM) [19,20]. The specimens were quickly and easily assembled for each test
393 and required no skilled or time-consuming labor.



(a) Loading jack and specimen in the laboratory

(b) Loading conditions of Test 1 to Test 4

394

Fig. 12: Test setup

395

Table 2: Description of test specimens

Test #	Loading condition			Specimen sizes*	
	Loads at connection	Point Loads	Moment to shear ratio (m)	Beams	Angles
1	Pure bending	2	N.A.	W18×46	L2½×2×3/8
2	Bending plus shear	1	1.84	W18×46	L2½×2×3/8
3	Bending plus shear	1	0.61	W21×57	L3×2×3/8
4	Bending plus shear	2	0.61	W21×57	L3×2×3/8

396

* US designations for hot rolled steel shapes

397

Fig. 13 shows the results of all four tests in terms of load-displacement curves, where load

398

was recorded in the loading jack and the vertical displacement was recorded at the connection

399

location. Results showed that, in all cases, the specimens with intermeshed steel connection

400

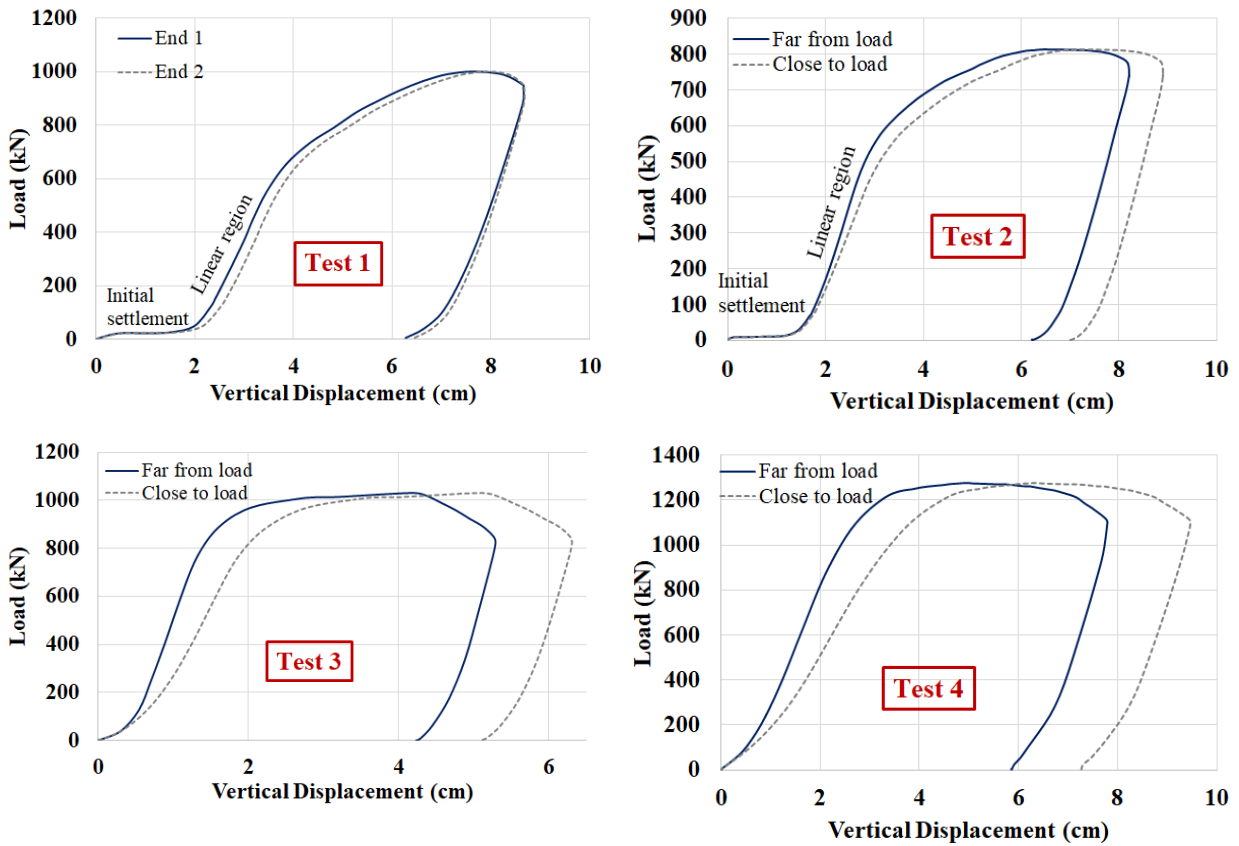
exhibited ample load carrying capacity and ductility. Table 3 summarizes some of the experimental

401

results in terms of performance criteria such as deformability, capacity, and stiffness. In this table,

402 the deformability is defined as the ratio of the displacement at the peak load (Δ_p) over the
 403 displacement at which the specimen starts yielding (Δ_y). Results show a displacement ratio range
 404 of 2.7 to 3.9, which shows the ability of the specimens to undergo significant plastic deformation
 405 before reducing peak load. While showing excellent deformability, the specimens exhibited ample
 406 load resistance, as the generated loads in the specimens were as high as 0.77 to 0.95 of M_p , the
 407 plastic moment capacity of the beam sections. This confirms that load could be transferred in the
 408 intermeshed steel connection via direct contact of different parts and without using welding or
 409 major bolting. Thus, beams with intermeshed steel connections can resist gravity loads expected
 410 in typical moment frames.

411



412 Fig. 13: Load at jack versus vertical displacement at connection ends for Test 1 to Test 4

413

414 On the other hand, Table 3 illustrates that the stiffness of the specimens (K_s) was a fraction
415 of the stiffness of the corresponding beam without the intermeshed connection (K_b). Another
416 words, installation of the intermeshed connection in a continuous steel beam causes a reduction in
417 the elastic stiffness of the beam, which could be as large as 47 to 76 percent. This is due to the
418 discontinuity at the connection region. Although closing the specimen gaps in the loading process
419 helps with stiffness formation, not all gaps will close completely and there will still be some
420 contacts that are not fully established. As a result, the intermeshed connection cannot attain the
421 ultimate beam stiffness and it only provides a fraction of that value. This stiffness loss might raise
422 some concerns for the application of the intermeshed system in steel moment frames. However,
423 results of Section 3 of this paper showed that when the intermeshed connection is located away
424 from the beam ends, the reduction in connection stiffness has no major effect on the stress or
425 deflection responses of the frame.

426

427

428

429

Table 3: Summary of the test results

Test #	Deformability* (Δ_p / Δ_y)	Load Capacity (M_{max} / M_p)	Initial Stiffness* (K_s / K_b)
1	3.8	0.77	0.50
2	3.9	0.94	0.53
3	3.3	0.95	0.45
4	2.7	0.88	0.24

430

* Not including the 'initial settlement' region of Tests 1 and 2

431 In all four tests, the specimen started to exhibit out-of-plane movement, and eventually
432 failed due to lateral-torsional buckling. This is because in the late stages of loading, the specimens
433 experienced high plasticity which caused a significant reduction in the material stiffness and
434 subsequently in sectional and member stiffness. Fig. 14 shows the specimens after the test was
435 completed. As can be seen, the out-of-plane failure mode was a product of pure lateral buckling
436 (Test 2 and Test 4) or a combination of lateral and torsional buckling (Test 1 and Test 3). In any
437 case, out-of-plane deflection occurred somewhere between the lateral braces and caused the
438 specimen to lose its load bearing ability. Thus, the bracing design was modified as the program
439 progressed from one test to the next due to the need for additional lateral restraint.



(a) Test 1



(b) Test 2



(c) Test 3 (d) Test 4
Fig. 14: Failure of the specimens due to lateral-torsional buckling

440
441
442
443
444
445
446
447
448
449
450
451
452
453
454
455
456
457
458
459
460
461

Fig. 13 shows an almost flat initial branch in the load-deflection curves of Tests 1 and 2, which is labeled as ‘initial settlement’. During this phase, the first and second specimens, respectively, deflected 2 cm and 1.3 cm under small loads, as a result of the very small stiffness. Visual observations during the tests showed that in this stage of loading, the ‘teeth and sockets’ were moving towards each other and the ‘bolts and shear plates’ were slipping towards one another. In fact, the full stiffness of the specimen was not formed until different connection elements came into contact and, subsequently, engaged in the load resistance.

While the initial settlement was relatively large in first two tests, this phenomenon was minimal in Tests 3 and 4, and those specimens began picking up load almost immediately after the test started (see Fig. 13). The reason is that, in the last two tests, the intermeshed connections were placed near the specimen end, and therefore a shorter lever arm was formed. In these specimens, gaps closed faster since the horizontal movement is a function of the lever arm length.

As it is illustrated in Fig. 4b, the intermeshed connection was established based on the premise of being placed at beam ends in a steel moment frame. Therefore, the initial settlement is not a concern for practicality of this system, as it would be small in that configuration. In any case, there exist some practical ways to control the deflections in a frame with intermeshed connections if needed. For instance, some camber could be introduced to eliminate deflections from floor deck weight. Tighter tolerances could also be used in the connection region, as the assembly process definitely showed some leeway in fitting all the connection parts together.

462 6. CONCLUSIONS

463 This study analyzed a radically new connection for structural steel members, which uses
464 multi-degree of freedom, volumetric cutting to reduce fabrication costs and vastly simplify and
465 speed erection. These fully automated cutting techniques could enhance the fabrication process
466 and consequently increase the productivity of construction. Based on this concept, two different
467 alternatives of intermeshed connection were proposed and investigated via finite element modeling
468 in Abaqus and experimental examination in laboratory.

469 Results showed that the front-intermeshed connection exhibits excellent shear resistance
470 but axial and flexural behavior are affected by the alignment of the intermeshed flanges. Based on
471 the flexural characteristics of the connection, the front-intermeshed connection shows low stiffness
472 and resistance rendering it a simple connection. For these reasons, this version of the intermeshed
473 connection was not pursued further in this study.

474 In keeping with the intermeshed connection concept, another alternative is proposed that
475 offers larger load capacity potential and larger erection tolerances. The resulting side-intermeshed
476 connection was designed, fabricated, and tested in the laboratory. Python X Robotic CNC plasma
477 and OMAX A-Jet waterjet cutting machines could successfully meet the required precision of the
478 intermeshed connection, determined in the design process. The results of experimental study on
479 four samples demonstrated high load carrying capacity as well as ample ductility and stiffness. All
480 four specimens failed due to lateral-torsional buckling, even though the lateral restraining system
481 was improved from Test 1 to Test 4. However, in real practice, the lateral-torsional buckling of
482 this system would be of much lesser concern, since the top flanges are usually restrained by a deck.

483

484 7. ACKNOWLEDGMENTS

485 The authors gratefully acknowledge the financial support provided by National Science
486 Foundation (NSF) through the grant CMMI-1563115, by Science Foundation Ireland through
487 grant SFI/15/US/B3234, by the Department for the Economy (DfE) and Invest Northern Ireland
488 (InvestNI) through grant USI-096, and by Enterprise Ireland through grant CF20160454. The
489 authors are very grateful to the American Institute for Steel Construction (AISC) for donating the
490 steel beams, angles and plates that were used to build the test specimens. The authors also express
491 their appreciation to the Department of Civil, Environmental, and Geo-Engineering at the
492 University of Minnesota for providing the fourth author (Ramzi Labbane) a departmental
493 fellowship. Lastly, the authors would like to thank Grunau Metals and Am-Tec Designs, the
494 manufacturers that fabricated the beams and angles, respectively.

495

496 8. REFERENCES

- 497 [1] S. Ramakrishnan, M. Gershenzon, F. Polivka, T.N. Kearney, M.W. Rogozinski, Plasma
498 generation for the plasma cutting process, IEEE Trans. PLASMA Sci. 25 (1997) 937–947.
- 499 [2] N.D. Perreira, R.B. Fleischman, B. V Viscomi, L.-W. Lu, Automated Construction and
500 ATLSS Connections; Development, Analysis, Experimentation, and Implementation of
501 ATLSS Connections for Automated Construction, 1993.
- 502 [3] McKinsey Global Institute, Reinventing Construction: A Route to Higher Productivity,
503 2017.
- 504 [4] D. Krajcarz, Comparison Metal Water Jet Cutting with Laser and Plasma Cutting, Procedia

- 505 Eng. 69 (2013) 838–843. doi:10.1016/j.proeng.2014.03.061.
- 506 [5] BOC Linde group, Facts about plasma technology and plasma cutting, 2011.
- 507 [6] L. Dahil, I. Dahil, A. Karabulut, Comparison of Advanced Cutting Techniques on Hardox
508 500 Steel Material and the Effect of Structural Properties of the Material, *Metalurgia*. 53
509 (2014) 291–294.
- 510 [7] S.A. Al Sabah, D.F. Laefer, GB Patent Application No 1718744.4, 2017.
- 511 [8] P. Matis, T. Martin, P. McGetrick, D. Robinson, The effect of frictional contact properties
512 on intermeshed steel connections, in: *Civ. Eng. Res. Irel., Civil Engineering Research in*
513 *Ireland, Dublin, 2018: pp. 547–553.*
- 514 [9] D. Systems, Abaqus 6.13, (2013).
- 515 [10] American Institute for Steel Constructions, Specification for Structural Steel Buildings,
516 2016.
- 517 [11] Eurocode, Eurocode 3: Design of steel structures - Part 1-8: Design of joints, 2005.
- 518 [12] S.A. Al Sabah, D.F. Laefer, GB Patent Application No 1718746.9, 2017.
- 519 [13] J. Sikora, A Summary of Stress Concentrations in the Vicinity of Openings in Ship
520 Structures, DAVID W TAYLOR Nav. Sh. Res. Dev. Cent. BETHESDA MD Struct. DEPT.
521 (1973).
- 522 [14] AISC, Steel Construction Manual, 15th Ed., American Institute of Steel Construction, 2017.
- 523 [15] American Institute of Steel Construction, Seismic Provisions for Structural Steel Buildings,
524 2016.

- 525 [16] P. McGetrick, T. Martin, P. Matis, D.F. Laefer, S. Al-Sabah, L. Truong-Hong, M.P. Huynh,
526 A.E. Schultz, J.-L. Le, M.E. Shemshadian, R. Labbane, The AMASS Project: Advanced
527 Manufacturing and Assembly of Steel Structures (submitted), Struct. Build. J. (2019).
- 528 [17] www.omax.com, Cutting Material with an Abrasive Waterjet, (2019).
529 <https://www.omax.com/frequently-asked-questions>.
- 530 [18] S. Al-Sabah, D. Laefer, L. Truong Hong, M.P. Huynh, J.-L. Le, T. Martin, P. Matis, P.
531 McGetrick, M.E. Schultz, Arturo Shemshadian, R. Dizon, Introduction of the Intermeshed
532 Steel Connection - A New Universal Steel Connection (submitted), Build. J. (2019).
- 533 [19] ASTM, ASTM A992 / A992M: Standard Specification for Structural Steel Shapes, 11
534 (2014) 11–14.
- 535 [20] ASTM, ASTM A36/A36M - Standard Specification for Carbon Structural Steel, (2018).
536